Aberrant Accumulation of Undifferentiated Myeloid Cells in the Adipose Tissue of CCR2-Deficient Mice Delays Improvements in Insulin Sensitivity

Dario A. Gutierrez, Arion Kennedy, Jeb S. Orr, Emily K. Anderson, Corey D. Webb, William K. Gerrald, and Alyssa H. Hasty

OBJECTIVE—Mice with CCR2 deficiency are protected from insulin resistance but only after long periods of high-fat diet (HFD) feeding, despite the virtual absence of circulating inflammatory monocytes. We performed a time course study in mice with hematopoietic and global CCR2 deficiency to determine adipose tissue–specific mechanisms for the delayed impact of CCR2 deficiency on insulin resistance.

RESEARCH DESIGN AND METHODS—Mice with global or hematopoietic CCR2 deficiency ($CCR2^{-/-}$ and BM-$CCR2^{-/-}$, respectively) and wild-type controls ($CCR2^{+/+}$ and BM-$CCR2^{+/+}$, respectively) were placed on an HFD for 6, 12, and 20 weeks. Adipose tissue myeloid populations, degree of inflammation, glucose tolerance, and insulin sensitivity were assessed.

RESULTS—Flow cytometry analysis showed that two different populations of $F4/80^{+}$ myeloid cells ($CD11b^{lo}F4/80^{lo}$ and $CD11b^{hi}F4/80^{hi}$) accumulated in the adipose tissue of $CCR2^{-/-}$ and BM-$CCR2^{-/-}$ mice after 6 and 12 weeks of HFD feeding, whereas only the $CD11b^{hi}F4/80^{hi}$ population was detected in the $CCR2^{+/+}$ and BM-$CCR2^{+/+}$ controls. After 20 weeks of HFD feeding, the $CD11b^{lo}F4/80^{lo}$ cells were no longer present in the adipose tissue of $CCR2^{-/-}$ mice, and only then were improvements in adipose tissue inflammation detected. Gene expression and histological analysis of the $CD11b^{lo}F4/80^{lo}$ cells indicated that they are a unique undifferentiated monocytic inflammatory population. The $CD11b^{lo}F4/80^{lo}$ cells are transiently found in wild-type mice, but CCR2 deficiency leads to the aberrant accumulation of these cells in adipose tissue.

CONCLUSIONS—The discovery of this novel adipose tissue monocytic cell population provides advances toward understanding the pleiotropic role of CCR2 in monocyte/macrophage accumulation and regulation of adipose tissue inflammation. ***Diabetes*** **60:2820–2829, 2011**

Obesity is an independent risk factor for type 2 diabetes, cardiovascular disease, fatty liver disease, atherosclerosis, and several cancers. Chronic adipose tissue inflammation is a cardinal feature of obesity that leads to other health complications such as insulin resistance (1–3). Recruitment of macrophages is an important factor in adipose tissue inflammation (4) and has been shown to be temporally associated with insulin resistance (5,6).

CCR2 regulates monocyte chemotaxis through direct interactions with its ligands, monocyte chemoattractant protein (MCP)-1 and -3 (7). $CCR2^{-/-}$ mice have an immune deficiency in Th1 responses characterized by low levels of interferon-γ (IFN-γ) production and delayed macrophage recruitment to sites of inflammation (8). A study by Tsou et al. (9) found that $CCR2^{-/-}$ mice have a defect in the egress of inflammatory monocytes from the bone marrow, resulting in a dramatic reduction of these cells in the circulation (9,10). Thus, $CCR2^{-/-}$ mice have a decreased pool of circulating inflammatory monocytes and reduced numbers of differentiated myeloid cells recruited to sites of inflammation.

The role of CCR2 and MCP-1 in macrophage recruitment to adipose tissue and the liver and their contribution to insulin resistance have been evaluated by various groups (11–16). One study showed that obese $CCR2^{-/-}$ mice have a modest decrease in macrophage marker expression and macrophage number in adipose tissue after 24 weeks on a 60% fat diet compared with wild-type controls (11). Furthermore, a bone marrow transplant (BMT) study showed that hematopoietic CCR2 deficiency leads to decreased F4/80 expression in the adipose tissue of obese *ob/ob* mice (13). These experiments indicate that substantial obesity (i.e., long periods of high-fat diet [HFD] feeding and/or a genetically morbidly obese model) is required before differences in macrophage recruitment and improvements in insulin sensitivity are observed in $CCR2^{-/-}$ mice, despite their striking reduction in circulating inflammatory monocytes. We set out to investigate the mechanism responsible for the delayed protection in adipose tissue inflammation and macrophage recruitment in global and hematopoietic models of CCR2 deficiency ($CCR2^{-/-}$ and BM-$CCR2^{-/-}$, respectively).

In this study, we analyzed the changes in myeloid populations that take place in the adipose tissue of $CCR2^{-/-}$ and BM-$CCR2^{-/-}$ mice during HFD-induced obesity and contrasted them with changes in $CCR2^{+/+}$ and BM-$CCR2^{+/+}$ controls. Our data showed that global and hematopoietic CCR2 deficiency leads to the accumulation of $CD11b^{lo}F4/80^{lo}$ myeloid cells during early periods of HFD feeding. Further analysis of the $CD11b^{lo}F4/80^{lo}$ cells showed that they have a monocytic and inflammatory gene expression profile characterized by significantly elevated expression of *Itgax*, *Il8rb*, *Ccl5*, *Nos2*, and *Csf1*. In addition, no differences in inflammation or glucose tolerance were observed between BM-$CCR2^{+/+}$ and BM-$CCR2^{-/-}$ mice until after substantial obesity was reached during extended periods of HFD feeding—a condition that corresponds temporally with the absence of $CD11b^{lo}F4/80^{lo}$ cells.

From the Department of Molecular Physiology and Biophysics, Vanderbilt School of Medicine, Nashville, Tennessee.
Corresponding author: Alyssa H. Hasty, alyssa.hasty@vanderbilt.edu.
Received 8 March 2011 and accepted 31 July 2011.
DOI: 10.2337/db11-0314
This article contains Supplementary Data online at http://diabetes.diabetesjournals.org/lookup/suppl/doi:10.2337/db11-0314/-/DC1.

RESEARCH DESIGN AND METHODS

All animal procedures were performed with approval from the Institutional Animal Care and Usage Committee of Vanderbilt University. The CCR2$^{-/-}$ and CCR2$^{+/+}$ mice used for the studies were originally purchased from The Jackson Laboratory, are on a C57BL/6 background, and have been propagated in our animal facility. All studies were performed with male 8-week-old mice. Mice were fed ad libitum and given free access to water. In the BMT study, mice were kept on antibiotic water from 1 week prior to BMT through 4 weeks post-BMT. Mice were then placed on a 60% HFD from Research Diets (D12492).

Bone marrow transplantation. Bone marrow cells were collected from CCR2$^{+/+}$ or CCR2$^{-/-}$ donor mice and were injected into the retro-orbital venous plexus of lethally irradiated recipient CCR2$^{+/+}$ mice as previously described (17). The efficiency of bone marrow reconstitution was confirmed by PCR using DNA isolated from the spleens of the recipient mice (data not shown).

Body weight, body composition, and food intake. Body weight and food intake were measured weekly for the duration of the study. Total lean, fat, and free fluid mass were measured by nuclear magnetic resonance using a Bruker Minispec (Woodlands, TX) in the Vanderbilt Mouse Metabolic Phenotyping Center at baseline and 6, 12, and 20 weeks after placement on an HFD.

Glucose and insulin tolerance tests. Mice were fasted for 5 h and baseline glucose levels measured using a LifeScan One Touch Ultra glucometer (Johnson & Johnson, Northridge, CA) via the tail vein. Mice were then injected intraperitoneally with glucose at 2 g/kg lean body mass for the 6-week mice and 1 g/kg lean body mass for the 12- and 20-week mice (glucose tolerance tests [GTTs]) or insulin at 0.4 units/kg lean body mass for the 6-week mice and 0.5 units/kg lean body mass for the 12- and 20-week mice (insulin tolerance tests [ITTs]). (13). Glucose levels were assessed at 15, 30, 45, 60, and 90 min after injection.

Plasma collection and measurements. Mice were fasted for 5 h before all blood collections and at sacrifice. Mice were bled from the retro-orbital venous plexus using heparinized collection tubes. Plasma was separated by centrifugation and stored at −80°C. Insulin levels were measured using an ELISA kit from Millipore (Billerica, MA).

Real-time RT-PCR. RNA extraction and cDNA Synthesis were performed as described previously (18). The reactions were carried out using IQ Supermix (BioRad) and FAM-conjugated Assay-on-Demand (Applied Biosystems, Foster City, CA) primer/probe sets normalized to glyceraldehyde-3-phosphate dehydrogenase. Catalog numbers will be provided upon request. Data were analyzed using the Pfaffl method (19) and presented as relative expression.

Adipose tissue lysates. The epididymal fat pads were collected at the end of the study, flash-frozen, and kept at −80°C until used. Approximately 50 mg adipose tissue was homogenized in 250 μL lysis buffer. The protein concentration in the lysate was quantified using the Lowry method with samples diluted in 0.1 N NaOH, 0.1% SDS.

IFN-γ and interleukin-4 enzyme-linked immunosorbent assay. IFN-γ and interleukin-4 (IL-4) enzyme-linked immunosorbent assays (ELISAs) were performed on adipose tissue lysates using BD Biosciences OptEIA ELISA kits according to the manufacturer's instructions; 50 μg total protein per well was used.

Histology. Toluidine Blue O (TBO) staining was performed as previously described (18). Crown-like structures (CLS) from eight different fields per mouse were quantified. CD11b^{lo}F4/80^{lo}- and CD11b^{hi}F4/80^{hi}-sorted cells were cytospun onto slides and stained with hematoxylin-eosin (H-E).

Stromal vascular fraction separation. After being killed, mice were perfused with 10 mL PBS. Adipose tissue pads were then minced in 3 mL of 0.5% BSA in PBS and placed on ice. Subsequently, 3 mL of 2 mg/mL collagenase was added to the minced fat and incubated at 37°C for 20 min with shaking. The cell suspension was filtered through a 100-μm filter and then spun at 300*g* for 10 min to separate floating adipocytes from the stromal vascular fraction (SVF) pellet. The SVF pellet was then resuspended in 3 mL ACK lysis buffer and incubated at room temperature for 5 min for erythrocyte lysis. The cells were then washed twice with PBS.

Peritoneal cell collection. CCR2$^{+/+}$ and CCR2$^{-/-}$ mice were injected intraperitoneally with 3 mL of 2% thioglycollate solution. The mice were killed 72 h later, and the cells were collected by flushing the peritoneal cavity with 10 mL of 0.5% BSA in PBS. Cells were washed twice with fresh PBS before staining for flow cytometry.

Flow cytometry. Stromal vascular cells (SVCs) and blood cells were first incubated with Fc block for 5 min at room temperature, followed by incubation for 30 min at 4°C with the fluorophore-conjugated antibodies indicated as follows: F4/80-APC (eBioscience), Ly6C-FITC (BD Biosciences), CD11b-APC-Cy7 (BD Bioscience), CD11c-PeCy7 (BD Bioscience), and Ly6G-PE (BD Bioscience). DAPI (0.2 μg/mL) was added to each sample as a viability stain 10 min before flow cytometry. Samples were processed on either a MACSQuant analyzer (Miltenyi Biotech) or a 5 Laser LSRII machine in the Vanderbilt Flow Cytometry Core and data analyzed using FlowJo software. During the analysis, all DAPI-negative cells (live) were gated (Supplementary Fig. 9) and used for further analysis with the specific fluorophores.

Cell sorting. Cells were collected and stained as described above for the flow cytometry section. The cells were sorted using a FACSAria I sorter at the Vanderbilt flow cytometry core. The CD11b^{lo}F4/80^{lo} and CD11b^{hi}F4/80^{hi} populations were isolated for RNA expression and histological analysis.

Statistics. GraphPad Prism 4.0 software was used for all statistical analyses. Data were analyzed using two-tailed unpaired *t* tests to determine differences between two groups with one variable, one-way ANOVA when more than two measurements were compared, and two-way ANOVA to compare measurements with two different variables (i.e., GTTs and ITTs). Outliers were excluded from the data for each individual parameter if outside the range of the mean ± 2 SD, and $P \leq 0.05$ was considered significant.

RESULTS

Weight and adiposity. Four weeks after BMT, BM-CCR2$^{-/-}$ and BM-CCR2$^{+/+}$ mice were placed on an HFD for 6, 12, or 20 weeks. The recipient groups had similar weight gain, adiposity, and epididymal fat pad weight throughout the study (Supplementary Fig.1). In addition, there were no differences in food intake between groups (data not shown).

Immunophenotype of circulating monocytes. BM-CCR2$^{-/-}$ mice fed an HFD for 12 weeks had a sevenfold reduction ($P < 0.001$) in the percentage of circulating Ly6C^{hi} monocytes (Supplementary Fig. 2*A–C*) compared with the BM-CCR2$^{+/+}$ mice. In addition, there was a significant increase in the levels of Ly6C^{lo} monocytes in the BM-CCR2$^{-/-}$ mice compared with the controls ($P < 0.01$) (Supplementary Fig. 2*D*). CCR2$^{-/-}$ mice fed an HFD for 12 weeks presented a similar reduction in Ly6C^{hi} monocytes compared with CCR2$^{+/+}$ controls (Supplementary Fig. 3*A* and *E*). We also analyzed the expression of CD11c, F4/80, and Ly6G in blood monocytes of CCR2$^{+/+}$ and CCR2$^{-/-}$ mice fed either an HFD or chow diet for 12 weeks (Supplementary Figs. 3 and 4). Interestingly, the Ly6C^{lo} population from HFD-fed CCR2$^{-/-}$ mice had increased CD11c expression (rightward shift of blue line in Supplementary Fig. 3*F*) compared with the Ly6C^{lo} cells from HFD-fed CCR2$^{+/+}$ mice (Supplementary Fig. 3*B*). In the general interest of assessing the effects of HFD feeding on the immunophenotype of circulating monocytes, we investigated monocytes isolated from HFD- and chow-fed CCR2$^{+/+}$ mice. When comparing the Ly6C^{hi} and Ly6C^{lo} populations in HFD-fed CCR2$^{+/+}$ mice, we found that the Ly6C^{hi} cells have a higher expression of CD11c (Supplementary Fig. 3*B*). In addition, as previously shown (20,21), a comparison of HFD- and chow-fed CCR2$^{+/+}$ mice showed increased expression of CD11c in Ly6C^{hi} monocytes, whereas the expression of CD11c in Ly6C^{lo} monocytes remained unaffected during HFD feeding (Supplementary Fig. 4*B* and *F*).

Glucose tolerance and insulin sensitivity. To examine the systemic metabolic effects of CCR2 deficiency, we performed GTTs and ITTs. We found no differences in glucose or insulin tolerance between groups at the 6- or 12-week time points (Fig. 1*A–D*). However, a modest improvement in glucose tolerance was found in the BM-CCR2$^{-/-}$ mice ($P < 0.05$), 15 min post-glucose injection, after 20 weeks of HFD feeding (Fig. 1*E*). Fasting glucose and insulin levels were not different between groups at any time (Table 1). Similar results were obtained in the global CCR2$^{-/-}$ mice, in which differences in glucose tolerance were not observed until after 20 weeks of HFD feeding (Supplementary Fig. 5*A–C*). The discrepancy in glucose tolerance between the hematopoietic and global CCR2-deficient models can be attributed to the reduced ability of mice

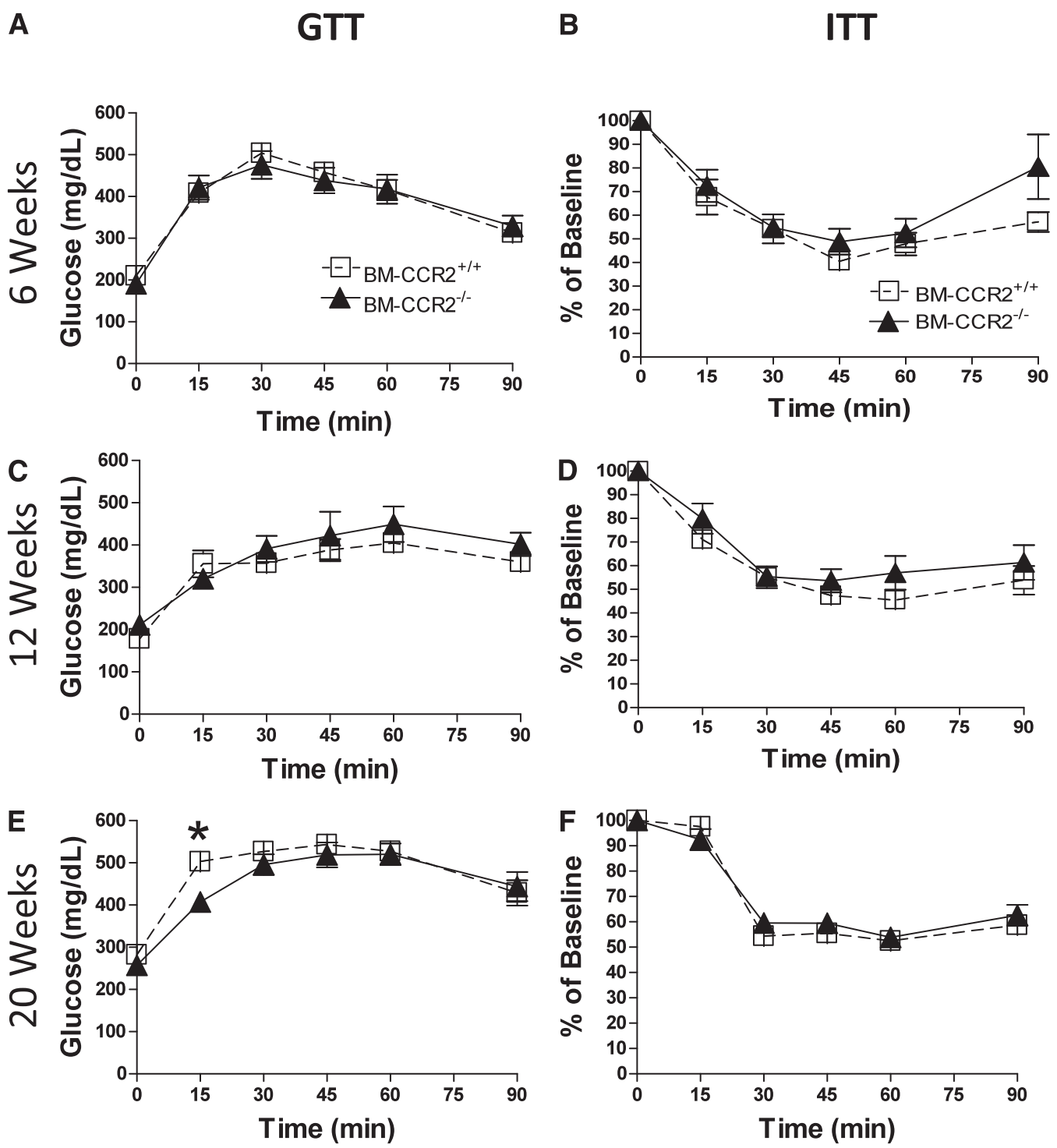

FIG. 1. BM-CCR2$^{-/-}$ mice have a modest improvement in glucose tolerance after extended periods of HFD feeding. All GTT (*left panels*) and ITT (*right panels*) experiments were performed by injecting mice with dextrose or insulin, at doses described in RESEARCH DESIGN AND METHODS, after a 5-h morning fast. *A*: GTT after 6 weeks of HFD feeding (mean ± SEM; *n* = 8–10 mice per group). *B*: ITT after 6 weeks of HFD feeding (mean ± SEM; *n* = 4–5 mice per group). *C*: GTT after 12 weeks of HFD feeding (mean ± SEM; *n* = 3–5 mice per group). *D*: ITT after 12 weeks of HFD feeding (mean ± SEM; *n* = 7–10 mice per group). *E*: GTT after 20 weeks of HFD feeding (mean ± SEM; *n* = 8–9 mice per group). *F*: ITT after 20 weeks on an HFD (mean ± SEM; *n* = 9 mice per group). **P* < 0.05 compared with the BM-CCR2$^{+/+}$ group at the 15-min time point.

undergoing BMT to gain weight (22). On average, BM-CCR2$^{-/-}$ mice weighed <40 g after 20 weeks of HFD feeding, whereas the CCR2$^{-/-}$ weighed >48 g during the same HFD feeding period.

Adipose tissue inflammatory state. Several reports indicate that CCR2$^{-/-}$ mice have deficient Th1 responses characterized by a low number of antigen-presenting cells, resulting in reduced levels of the Th1 cytokine IFN-γ (8,23) or elevated IL-4 (24). Assessment of IFN-γ and IL-4 in adipose tissue lysates from BM-CCR2$^{-/-}$ and BM-CCR2$^{+/+}$ mice showed no differences in these cytokines levels between groups after any period of HFD feeding (Supplementary Fig. 6*A* and *B*). Gene expression of the inflammatory genes *Tnf* and *Nos2* was not different between groups

TABLE 1
No differences in fasting insulin or glucose were detected between the BM-CCR2$^{+/+}$ and BM-CCR2$^{-/-}$ mice

	BM-CCR2$^{+/+}$	BM-CCR2$^{-/-}$
Insulin (ng/mL)		
6 weeks	0.54 ± 0.24	0.60 ± 0.19
12 weeks	0.98 ± 0.76	1.18 ± 1.27
20 weeks	1.50 ± 0.33	2.27 ± 0.67
Glucose (mg/dL)		
6 weeks	156 ± 29	178 ± 26
12 weeks	164 ± 20	180 ± 34
20 weeks	282 ± 51	257 ± 30

Data are means ± SEM. Fasting glucose levels were assessed after a 5-h morning fast. Fasting insulin was measured by ELISA (n = 7–10 mice per group).

at the 6- or 12-week time points (Supplementary Fig. 6*C* and *D*); however, *Tnf* expression was significantly lower ($P < 0.05$) in the BM-CCR2$^{-/-}$ mice after 20 weeks of HFD feeding (Supplementary Fig. 6*E*). Gene expression of the chemokines MCP-1 (*Ccl2*) and macrophage inflammatory protein-1α (*Ccl3*) was significantly increased after 6 ($P < 0.01$; $P < 0.001$) and 12 weeks ($P < 0.05$; $P < 0.01$) in the BM-CCR2$^{-/-}$ mice; no differences in the expression of these chemokines were observed in the mice fed an HFD for 20 weeks.

The BM-CCR2$^{-/-}$ mice presented a threefold increase in the expression of the anti-inflammatory marker arginase 1 (*Arg1*) at 6 and 12 weeks ($P < 0.01$); expression of this gene was not different between groups after 20 weeks of HFD feeding (Supplementary Fig. 6*C–E*). Expression of *Cd163*, *mgl1*, *mgl2*, and *Il10* was assessed, and no consistent changes were observed in these "M2" or anti-inflammatory genes between groups after any period of HFD feeding.

Immune cell infiltration into adipose tissue. CLS, which are an accumulation of immune cells around presumably dead adipocytes, were used to quantify immune cell infiltration in TBO-stained sections of adipose tissue (Fig. 2*A–F*). There were no differences in numbers of CLS between BM-CCR2$^{-/-}$ and BM-CCR2$^{+/+}$ mice after 6 or 12 weeks of HFD feeding (Fig. 2*G*). However, there was a significant decrease ($P < 0.05$) in CLS in the BM-CCR2$^{-/-}$ mice after 20 weeks of HFD feeding (Fig. 2*E–F*). Further analysis of TBO-stained adipose tissue from mice fed an HFD for 20 weeks showed that the number of CLS is dependent on the body weight of the mouse. There were no differences between weight-matched BM-CCR2$^{-/-}$ and BM-CCR2$^{+/+}$ mice when they weighed <40 g; conversely, there was a decrease in CLS in the BM-CCR2$^{-/-}$ mice compared with weight-matched BM-CCR2$^{+/+}$ controls at >45 g body weight (Supplementary Fig. 7). In accordance with our histological data, there were no differences in the expression of CD68 (*Cd68*), CD11b (*Itgam*), or CD11c (*Itgax*) in adipose tissue of BM-CCR2$^{-/-}$ compared with BM-CCR2$^{+/+}$ mice after 6 or 12 weeks of HFD feeding (Fig. 2*H* and *I*); however, the expression of these genes was significantly lower ($P < 0.05$) for the BM-CCR2 $^{-/-}$ mice by the 20-week time point compared with the control group (Fig. 2*J*). The expression of F4/80 (*Emr1*) in adipose tissue of BM-CCR2$^{-/-}$ mice was significantly ($P < 0.05$) increased after 6 weeks and unchanged after 12 weeks, and there was a trend ($P < 0.07$) toward a decrease after 20 weeks of an HFD in comparison with the BM-CCR2$^{+/+}$ controls (Fig. 2*H–J*).

CCR2 deficiency leads to the aberrant accumulation of F4/80^{lo} cells in adipose tissue. Based on our observation that there were no changes in immune infiltration in adipose tissue after 6 and 12 weeks of HFD feeding despite the dramatic reduction in circulating inflammatory cells, we sought to further characterize the macrophages in adipose tissue by flow cytometry. To this end, we performed careful evaluation of the F4/80^{+} cells within adipose tissue. Based on our gating strategy, the BM-CCR2$^{+/+}$ mice contained the expected F4/80^{-} and F4/80^{hi} populations (Fig. 3*A*). Interestingly, the BM-CCR2$^{-/-}$ mice accumulated two discrete myeloid populations in their adipose tissue: F4/80^{lo} and F4/80^{hi} (Fig. 3*B*). The discrete F4/80^{lo} population was observed in the SVF of the BM-CCR2$^{-/-}$ at the 6-week (Fig. 3*B* and *C*) and 12-week (Fig. 3*C* and Supplementary Fig. 8*B*) time points but was no longer detected after 20 weeks of HFD feeding (Fig. 3*C* and Supplementary Fig. 8*D*).

Real-time RT-PCR analysis of RNA isolated from whole adipose tissue of BM-CCR2$^{-/-}$ mice showed that the presence of the F4/80^{lo} population at 6 and 12 weeks was associated with increases in gene expression of myeloperoxidase (*Mpo*) ($P < 0.05$), CXCR2 (*IL8rb*) ($P < 0.01$), *Cxcl1* ($P < 0.001$), and *Cxcl2* ($P < 0.05$) (Fig. 3*D* and *E*). No differences in the expression of these genes were observed after 20 weeks of an HFD, when the CD11b^{lo}F4/80^{lo} cells were no longer detected (Fig. 3*F*).

Similar to the analysis of the BM-CCR2$^{-/-}$ model, analysis of the SVCs of the CCR2$^{-/-}$ mice showed that CD11b^{lo}F4/80^{lo} cells aberrantly accumulate in the adipose tissue of global CCR2$^{-/-}$ mice with similar kinetics. The cells accumulated in the adipose tissue of CCR2$^{-/-}$ mice after 6 or 12 weeks of HFD feeding (Fig. 4*D* and *E*), whereas no discrete population was found in the CCR2$^{+/+}$ controls (Fig. 4*A* and *B*). Additionally, after 20 weeks of HFD feeding, the CD11b^{lo}F4/80^{lo} cells were no longer found in the adipose tissue of CCR2$^{-/-}$ mice (Fig. 4*F*). Note that there is downward shift of the double-positive populations in both the CCR2$^{+/+}$ and CCR2$^{-/-}$ mice after 20 weeks of HFD feeding (Fig. 4*C* and *F*). Identical flow conditions were used as in the earlier time points. Therefore, we hypothesize that the difference may be due to the excess lipid interference with signal detection; nonetheless, only one population of CD11b^{+}F4/80^{+} cells was found in both genetic models at this time point. Global CCR2$^{-/-}$ mice were used for subsequent characterization of the CD11b^{lo}F4/80^{lo} cells.

CD11b^{lo}F4/80^{lo} cell characterization. CD11b^{hi}F4/80^{hi} and CD11b^{lo}F4/80^{lo} cells were isolated from the adipose tissue of CCR2$^{-/-}$ mice 10 weeks post–HFD feeding (Fig. 5*A*). Gene expression analysis was performed for both populations and is presented as expression relative to the CD11b^{hi}F4/80^{hi} cells (Fig. 5*B*). Expression of *Emr1* ($P < 0.001$) was significantly lower for CD11b^{lo}F4/80^{lo} cells, as expected based on our gating strategy. The expression of *Arg1* ($P < 0.05$), *Cd163* ($P < 0.001$), *Il10* ($P < 0.01$), *Il6* ($P < 0.01$), *Ccr5* ($P < 0.05$), *Ccl2* ($P < 0.01$), and *Csfr1* ($P < 0.001$) was significantly lower in the CD11b^{lo}F4/80^{lo} cells in comparison with the CD11b^{hi}F4/80^{hi} macrophages. Expression of *Itgax* ($P < 0.01$), *Nos2* ($P < 0.05$), *Ccl5* ($P < 0.01$), *Il8rb* ($P < 0.05$), and *Csf1* ($P < 0.05$) was significantly higher for the CD11b^{lo}F4/80^{lo} cells. H-E staining of the sorted CD11b^{lo}F4/80^{lo} cells showed that these cells have a monocytic morphology and are smaller in size than the CD11b^{hi}F4/80^{hi} macrophages (Fig. 5*C*). Despite several reports of neutrophilia at sites of inflammation in

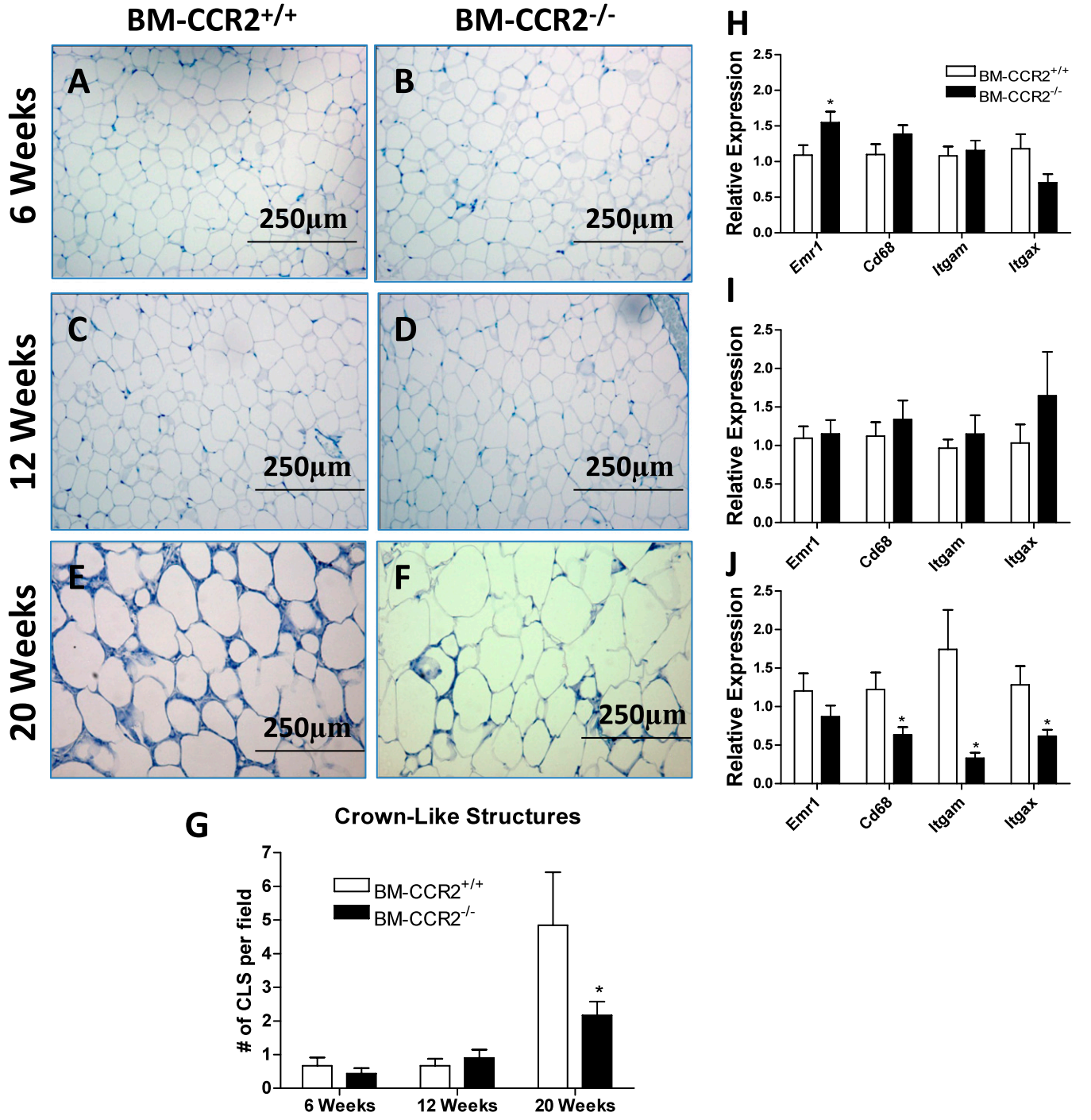

FIG. 2. BM-CCR2$^{-/-}$ mice have decreased immune infiltration and macrophage marker expression after extended periods of HFD feeding. Adipose tissue was collected from BM-CCR2$^{+/+}$ and BM-CCR2$^{-/-}$ mice fed an HFD for 6, 12, or 20 weeks and used to assess macrophage infiltration by histological and gene expression analysis. *A–F*: Representative TBO-stained images from mice as indicated. *G*: CLS in TBO-stained adipose tissue sections were quantified from eight different fields per mouse and presented as number of CLS per field (mean ± SEM; *n* = 5–7 mice per group). *H–J*: RNA was isolated from adipose tissue and used for gene expression analysis by real-time RT-PCR. The expression of the macrophage markers *Emr1*, *Cd68*, *Itgam*, and *Itgax* was assessed after 6, 12, and 20 weeks of HFD feeding and plotted as expression relative to the BM-CCR2$^{+/+}$ group of each time point (mean ± SEM; *n* = 7–10 mice per group). **P* < 0.05 compared with the 20-week BM-CCR2$^{+/+}$ group. (A high-quality color representation of this figure is available in the online issue.)

CCR2$^{-/-}$ mice (25,26), flow cytometry analysis of the CD11b^{lo}F4/80^{lo} population in the global CCR2$^{-/-}$ mice showed that these cells are Ly6G negative and therefore unlikely to be neutrophils (Supplementary Fig. 9).

CD11b^{lo}F4/80^{lo} cells are transiently found in CCR2$^{+/+}$ mice. To determine the physiological relevance of the CD11b^{lo}F4/80^{lo} cells in wild-type conditions, we isolated CD11b^{lo}F4/80^{lo} and CD11b^{hi}F4/80^{hi} macrophages from CCR2$^{+/+}$ mice fed an HFD for 7 weeks. Despite the absence of two discrete populations in the CCR2$^{+/+}$ mice, we were able to isolate CD11b^{lo}F4/80^{lo} cells and found that they have gene expression (Fig. 6*B*) and morphology (Fig. 6*C*) similar with the CD11b^{lo}F4/80^{lo} cells isolated from the adipose tissue of CCR2$^{-/-}$ mice. In addition, we assessed

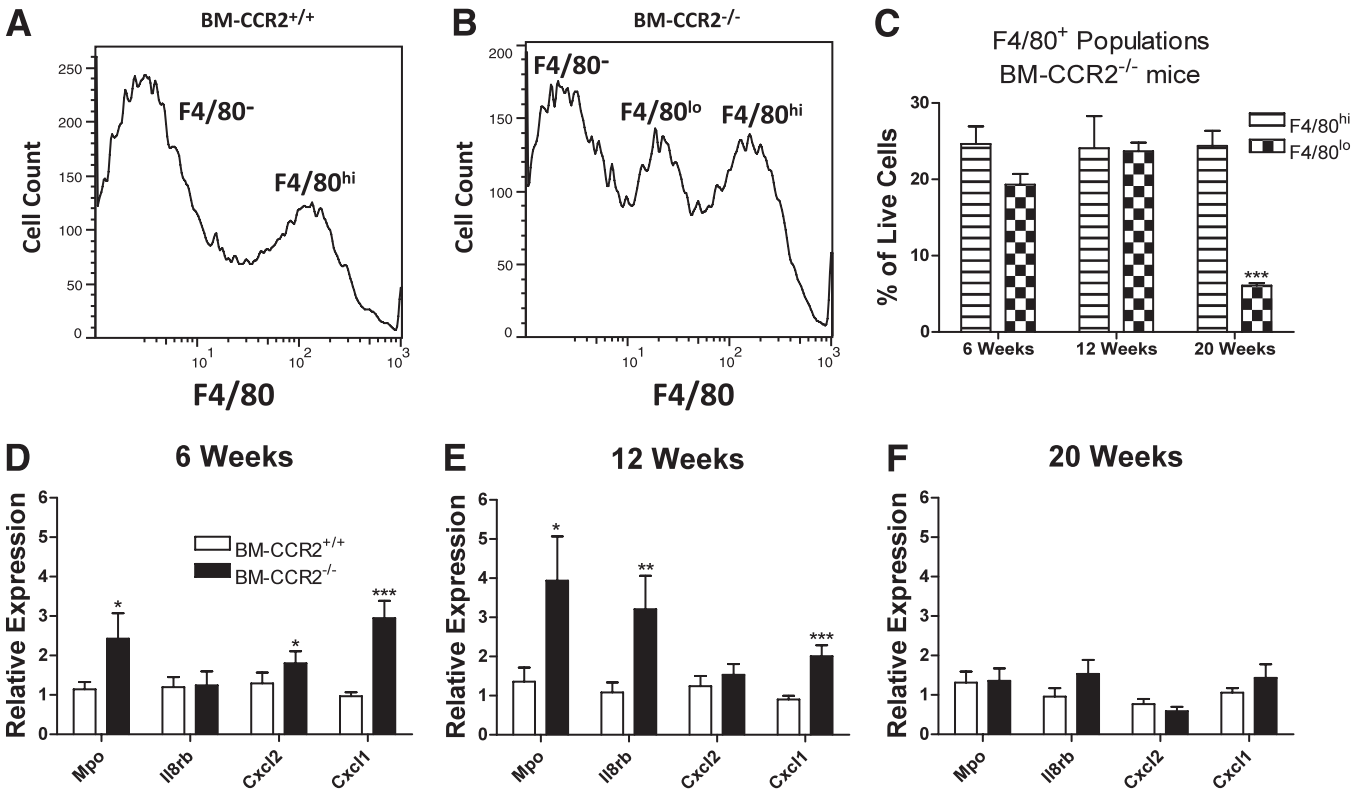

FIG. 3. A unique F4/80^{lo} myeloid population accumulates in the SVF of the adipose tissue of BM-CCR2$^{-/-}$ mice. SVCs isolated from BM-CCR2$^{+/+}$ and BM-CCR2$^{-/-}$ mice were analyzed by flow cytometry. Representative flow cytometry histogram of F4/80-expressing populations in a BM-CCR2$^{+/+}$ mouse (*A*) and in a BM-CCR2$^{-/-}$ mouse (*B*) gated on all live cells. *C*: Quantification of F4/80^{lo} vs. F4/80^{hi} cell percentages after 6, 12, and 20 weeks of an HFD in the BM-CCR2$^{-/-}$ mice (mean ± SEM; *n* = 3–5). *D–F*: RNA was isolated from adipose tissue and used for gene expression analysis by real-time RT-PCR. The mRNA expression of *Mpo*, *Il8rb*, *Cxcl2*, and *Cxcl1* was assessed after 6 (*D*), 12 (*E*), and 20 (*F*) weeks of HFD feeding and plotted as expression relative to the BM-CCR2$^{+/+}$ group of each time point (mean ± SEM; *n* = 7–10 mice per group). **P* < 0.05 compared with the BM-CCR2$^{+/+}$ group. ***P* < 0.01 compared with the BM-CCR2$^{+/+}$ group. ****P* < 0.001 compared with the BM-CCR2$^{+/+}$ group.

whether HFD feeding was necessary for the accumulation of CD11b^{lo}F4/80^{lo} cells. The expression of several key genes in the CD11b^{lo}F4/80^{lo} cells isolated from chow-fed CCR2$^{-/-}$ and CCR2$^{+/+}$ mice (Supplementary Fig. 10) was similar to that of CD11b^{lo}F4/80^{lo} cells isolated from the HFD mice (Figs. 5*B* and 6*B*).

CD11b^{lo}F4/80^{lo} aberrantly accumulate in the peritoneum of thioglycollate-injected CCR2$^{-/-}$ mice. To determine whether CD11b^{lo}F4/80^{lo} cells accumulated in other metabolic relevant tissues during obesity or in an acute model of inflammation, we assessed the accumulation of these cells in the livers of HFD-fed and thioglycollate-injected CCR2$^{-/-}$ mice, respectively. We did not observe the accumulation of these cells in livers of HFD-fed mice, but we found a decrease in the number of recruited inflammatory macrophages as recently shown by Obstfeld et al. (27) (data not shown). In contrast, we observed a marked aberrant accumulation of CD11b^{lo}F4/80^{lo} and a decrease in CD11b^{hi}F4/80^{hi} cells in the peritoneum of CCR2$^{-/-}$ mice compared with CCR2$^{+/+}$ mice at 72 h after thioglycollate injection (Supplementary Fig. 11).

DISCUSSION

CCR2$^{-/-}$ mice have been shown to have a modest reduction in macrophage recruitment to adipose tissue after extended periods of HFD feeding (11,13). Given that the pool of circulating inflammatory monocytes is strikingly reduced in these mice (9) (Supplementary Figs. 2*B* and *C* and 3*E*), inflammatory macrophage recruitment to adipose tissue should be correspondingly decreased. However, inflammation and inflammatory macrophage recruitment in CCR2$^{-/-}$ mice is only partially decreased and only after substantial obesity is attained (11,13). Our current studies explored mice with global and hematopoietic CCR2 deficiency at different periods of HFD feeding to investigate the mechanism involved in the delayed improvement in inflammation and insulin sensitivity.

To understand processes that take place at earlier stages of obesity that could prevent improvements in inflammation and insulin resistance, we analyzed myeloid populations in adipose tissue of BM-CCR2$^{-/-}$ and CCR2$^{-/-}$ mice and control mice after 6, 12, and 20 weeks of an HFD by flow cytometry. Our data provide evidence for the accumulation of a unique CD11b^{lo}F4/80^{lo} myeloid population in the adipose tissue of BM-CCR2$^{-/-}$ (Fig. 3*B* and *C* and Supplementary Fig. 8*B*) and CCR2$^{-/-}$ (Fig. 4*D* and *E*) mice after 6 and 12 weeks of HFD feeding. These CD11b^{lo}F4/80^{lo} cells are no longer detected in the adipose tissue of the BM-CCR2$^{-/-}$ or CCR2$^{-/-}$ mice after extended periods (>20 weeks) of HFD feeding (Figs. 3*C* and 4*C* and *F* and Supplementary Fig. 8*C* and *D*). Our data suggest that the presence of the CD11b^{lo}F4/80^{lo} cells is associated with the mechanism(s) for the delay in improvements in inflammation and insulin resistance observed in these mice and that substantial obesity and disappearance of the CD11b^{lo}F4/80^{lo} cells are required before metabolic improvements are attained.

To determine the identity and inflammatory phenotype of the novel CD11b^{lo}F4/80^{lo} cells, we isolated RNA from

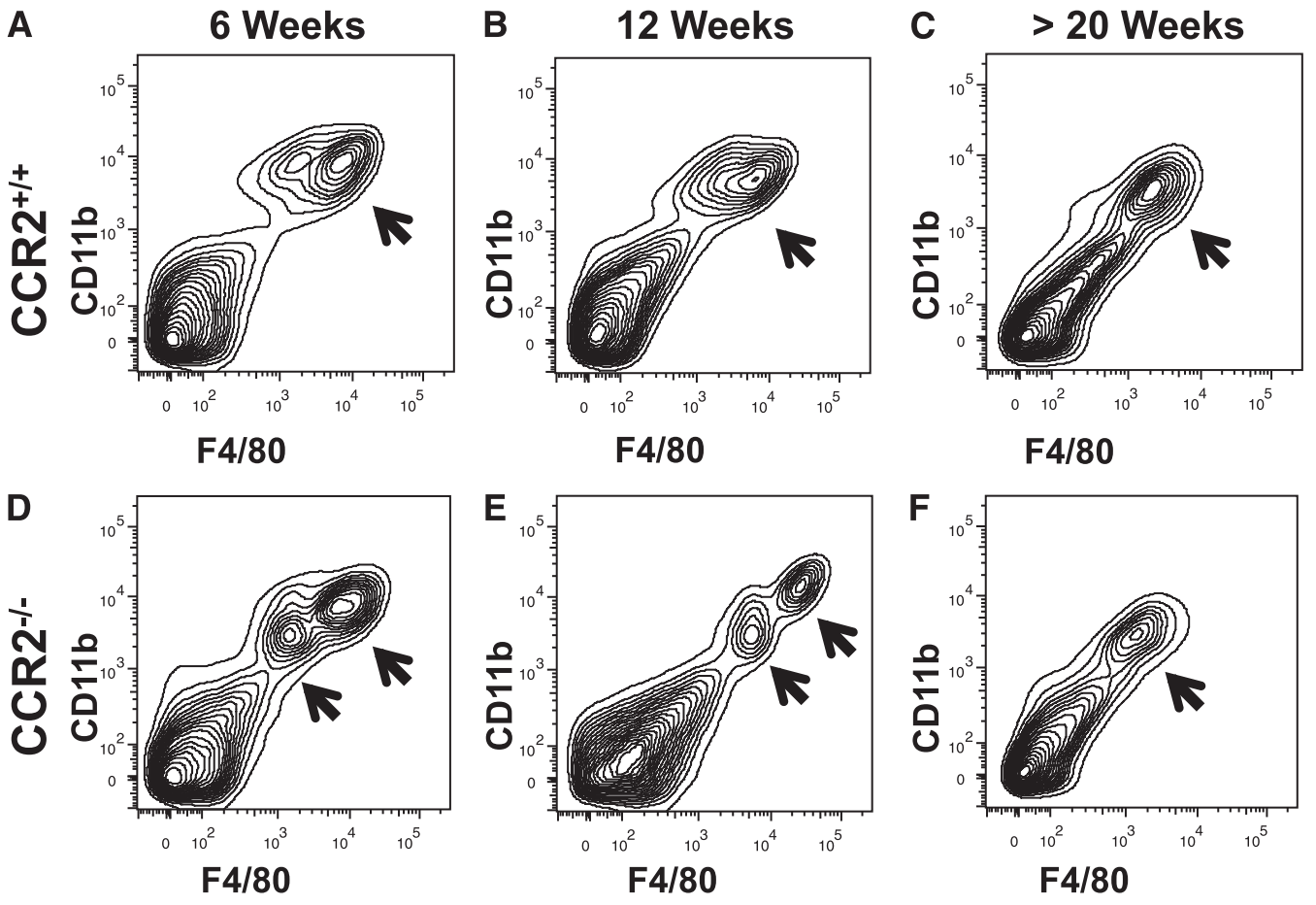

FIG. 4. CD11b^{lo}F4/80^{lo} cells accumulate in global CCR2$^{-/-}$ mice. Representative contour plots of F4/80 vs. CD11b expression in SVCs from CCR2$^{+/+}$ mice after 6 weeks (*A*), 12 weeks (*B*), and 20 weeks (*C*) on an HFD. Representative contour plots of F4/80 vs. CD11b expression in SVCs from CCR2$^{-/-}$ mice after 6 weeks (*D*), 12 weeks (*E*), and 20 weeks (*F*) on an HFD (n = 4 biological replicates).

these cells for gene expression characterization. Altogether, the expression data suggest that the CD11b^{lo}F4/80^{lo} cells do not exhibit classical M1 or M2 expression profiles but, instead, have a unique inflammatory expression in contrast with that of CD11b^{hi}F4/80^{hi} macrophages. Chomarat et al. (28) showed that during monocyte to macrophage differentiation there is an upregulation of CD115 (*Csf1r*) coupled by a downregulation of its ligand, M-CSF (*Csf1*). We measured the expression of both *Csfr1* and *Csf1* and found that *Csfr1* was downregulated while *Csf1* was upregulated in the CD11b^{lo}F4/80^{lo} cells, suggesting that they are in a monocytic transition stage. To test this, we found that CD11b^{lo}F4/80^{lo} cells have a monocytic morphology—in contrast with the CD11b^{hi}F4/80^{hi} cells, which have a morphology characteristic of macrophages (Fig. 5*C*). The expression profile and morphological analysis indicate that the CD11b^{lo}F4/80^{lo} cells are inflammatory monocytes that accumulate in adipose tissue in the absence of CCR2.

We also sought to investigate the presence of the CD11b^{lo}F4/80^{lo} cells in wild-type mice independent of CCR2 deficiency. We isolated CD11b^{lo}F4/80^{lo} and CD11b^{hi}F4/80^{hi} macrophages from CCR2$^{+/+}$ mice using identical gates as previously used for the CCR2$^{-/-}$ mice (Fig. 6*A*). Despite the absence of a discrete population under the CD11b^{lo}F4/80^{lo} (P2) gate, we were able to isolate a relatively high number of cells. Gene expression analysis of key markers of CD11b^{lo}F4/80^{lo} cells previously described showed that CD11b^{lo}F4/80^{lo} cells isolated from CCR2$^{+/+}$ mice have gene expression patterns identical with those of the CCR2$^{-/-}$ mice (Fig. 6*B*). Additionally, H&E staining of isolated cells showed a similar monocytic morphology between the CCR2$^{-/-}$ and CCR2$^{+/+}$ CD11b^{lo}F4/80^{lo} cells (Figs. 5*C* and 6*C*). Moreover, we found that HFD feeding was not necessary for the accumulation of these cells in adipose tissue; CD11b^{lo}F4/80^{lo} cells were found in chow-fed CCR2$^{+/+}$ and CCR2$^{-/-}$ mice (Supplementary Fig. 10). Next, we assessed whether these cells were found in the liver and the peritoneal cavity after thioglycollate injection. We did not observe their accumulation in the liver; however, we did observe the decrease in recruited macrophages without effects on resident Kupffer cells, as recently described by Obstfeld et al. (27) (data not shown). On the other hand, we found a marked accumulation of CD11b^{lo}F4/80^{lo} cells in the peritoneum of thioglycollate-injected CCR2$^{-/-}$ mice in comparison with CCR2$^{+/+}$ controls (Supplementary Fig. 11*A* and *B*). In addition, we were able to clearly observe the accumulation of the CD11b^{lo}F4/80^{lo} cell population in the CCR2$^{+/+}$ mice, albeit at lower levels than in the CCR2$^{-/-}$ mice (Supplementary Fig. 11*B*). These findings indicate that although CCR2 deficiency is not necessary for the recruitment of CD11b^{lo}F4/80^{lo} cells to adipose tissue and the peritoneum, it leads to the aberrant accumulation of these cells, which would otherwise only transiently be found at these inflammatory sites.

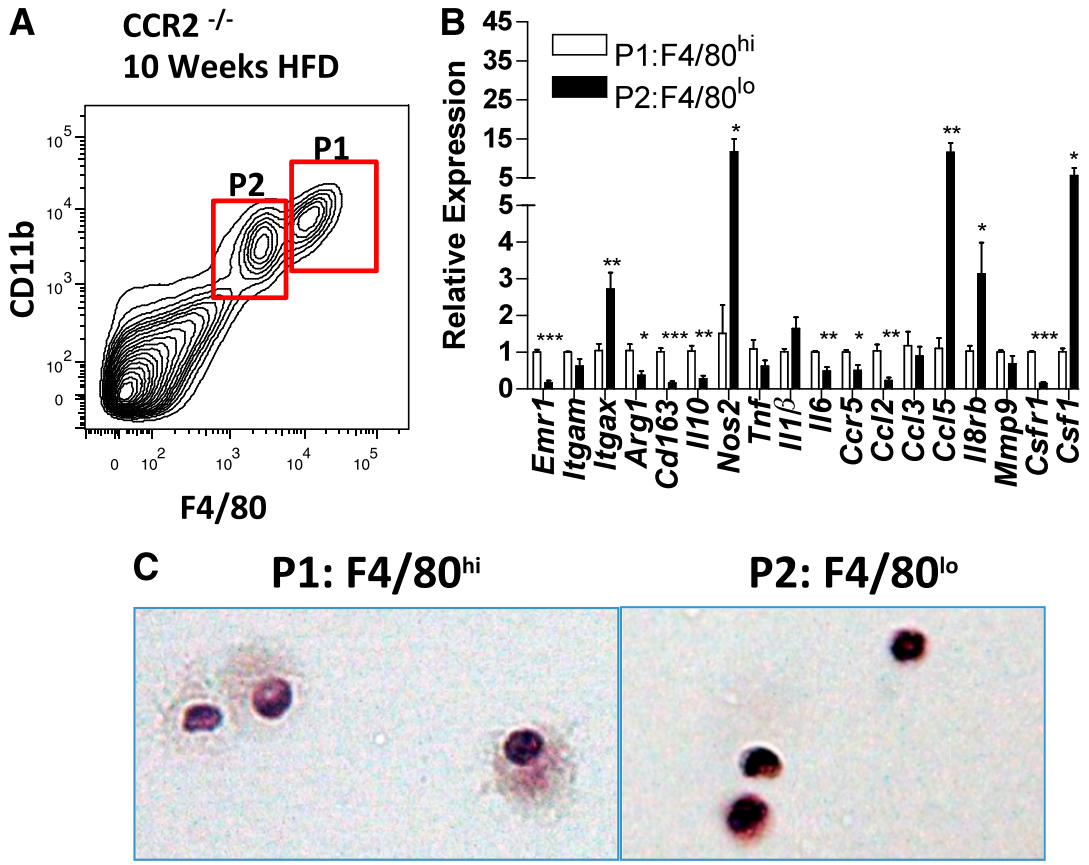

FIG. 5. CD11b^{lo}F4/80^{lo} cells have an inflammatory expression profile and a monocytic morphology. CD11b^{lo}F4/80^{lo} and CD11b^{hi}F4/80^{hi} cells were isolated by fluorescence-activated cell sorting from CCR2$^{-/-}$ mice fed an HFD for 10 weeks. *A*: Gating strategy used for cell sorting; CD11b^{hi}F4/80^{hi} (P1) and CD11b^{lo}F4/80^{lo} (P2). RNA was isolated from the sorted cells and used for gene expression analysis by real-time RT-PCR. *B*: Gene expression profiles in CD11b^{lo}F4/80^{lo} (P2) cells relative to CD11b^{hi}F4/80^{hi} (P1) cells in CCR2$^{-/-}$ mice were assessed (mean ± SEM; *n* = 4 biological replicates). *C*: Representative images of H-E–stained CD11b^{hi}F4/80^{hi} (P1) and CD11b^{lo}F4/80^{lo} (P2) cells. **P* < 0.05 compared with CD11b^{hi}F4/80^{hi}. ***P* < 0.01 compared with CD11b^{hi}F4/80^{hi}. ****P* < 0.001 compared with CD11b^{hi}F4/80^{hi}. (A high-quality color representation of this figure is available in the online issue.)

The mechanism for the accumulation and eventual disappearance of the CD11b^{lo}F4/80^{lo} cells is unknown. A recent study using antibody treatment against colony stimulating factor 1 receptor (CSFR1) resulted in the accumulation of inflammatory F4/80^{lo} myeloid cells and a decrease in the differentiated F4/80^{hi} macrophages in lymphoid tissues (29). CSFR1 is involved in the differentiation of monocytes to macrophages (28); thus, inhibition of this receptor led to the accumulation of undifferentiated monocytes (29). Similarly, CCR2 and its ligand CCL2 have been shown to play a role in monocyte to macrophage differentiation (30). Thus, it is possible that just as in CSFR1 antagonism, CCR2 deficiency leads to the aberrant accumulation of CD11b^{lo}F4/80^{lo} myeloid cells in adipose tissue. Accordingly, a possible mechanism for their disappearance is the eventual differentiation of the CD11b^{lo}F4/80^{lo} myeloid cells into CD11b^{hi}F4/80^{hi} macrophages in adipose tissue during advanced stages of obesity, when no active recruitment is taking place. Future studies will address the origin and mechanism(s) of recruitment and disappearance of the CD11b^{lo}F4/80^{lo} cells.

In conclusion, our data provide evidence for the aberrant accumulation of the novel CD11b^{lo}F4/80^{lo} myeloid cells in the adipose tissue of CCR2$^{-/-}$ mice, which is associated with delayed improvements in inflammation and glucose tolerance in this mouse model during obesity. We found that the CD11b^{lo}F4/80^{lo} cells are also found in the adipose tissue of CCR2$^{+/+}$ mice (albeit in lower numbers) and that an HFD is not required for their recruitment into adipose tissue. The gene expression and histological analysis of the CD11b^{lo}F4/80^{lo} cells indicate that these cells have a monocytic nature. In addition, their transient accumulation in the adipose tissue of CCR2$^{+/+}$ mice suggests that the CD11b^{lo}F4/80^{lo} cells are in a transition stage and that CCR2 is necessary for their differentiation into CD11b^{hi}F4/80^{hi} macrophages. Our study has provided in vivo evidence for the role of CCR2 in macrophage recruitment and differentiation in adipose tissue and has highlighted the metabolic consequences of the aberrant accumulation of undifferentiated CD11b^{lo}F4/80^{lo} cells in this tissue. The discovery of this potentially highly inflammatory myeloid population in the adipose tissue of CCR2$^{-/-}$ mice also has implications for the use of CCR2 antagonism as a therapy for chronic inflammatory diseases because it could worsen inflammation during early stages of the inflammatory process (31,32). Future and ongoing studies will investigate the role of these cells in different inflammatory settings.

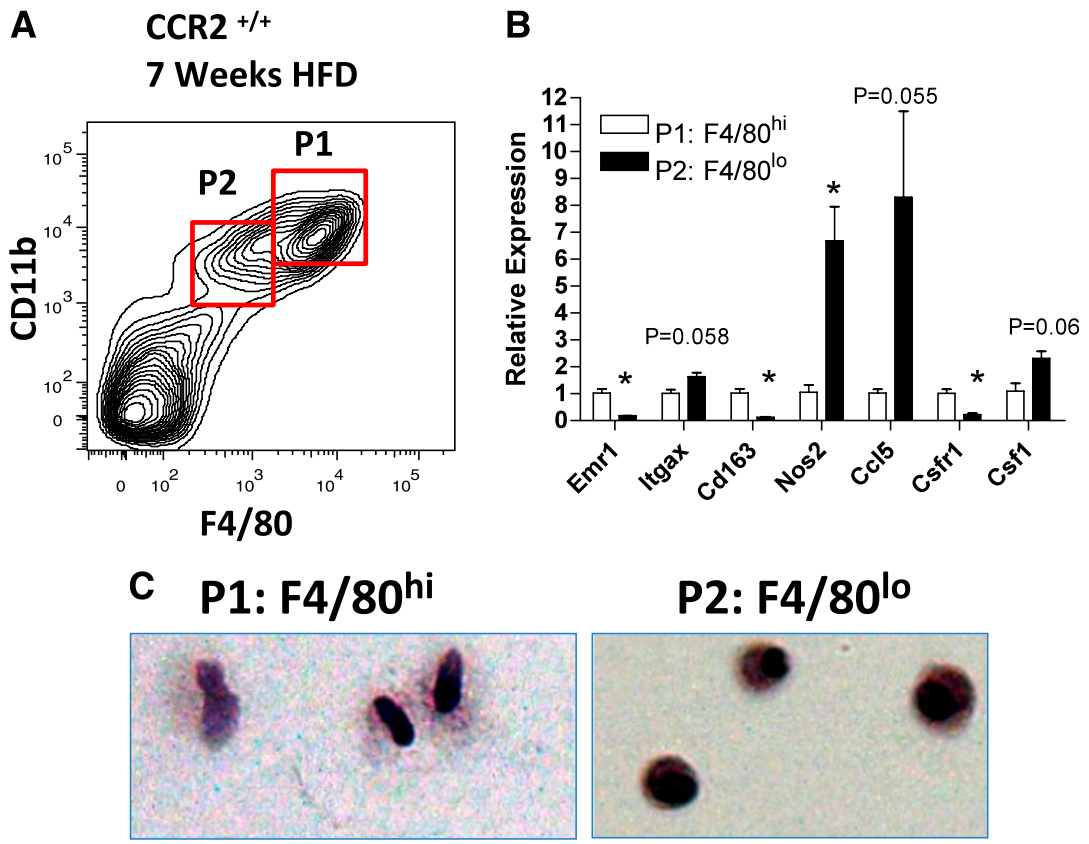

FIG. 6. CD11b^{lo}F4/80^{lo} cells are transiently found in the adipose tissue of HFD-fed CCR2$^{+/+}$ mice. CD11b^{lo}F4/80^{lo} and CD11b^{hi}F4/80^{hi} cells were isolated by fluorescence-activated cell sorting from CCR2$^{+/+}$ mice fed an HFD for 7 weeks. *A*: Gating strategy used for cell sorting; CD11b^{hi}F4/80^{hi} (P1) and CD11b^{lo}F4/80^{lo} (P2). RNA was isolated from the sorted cells and used for expression analysis of key CD11b^{lo}F4/80^{lo} genes by real-time RT-PCR. *B*: Gene expression profiles in CD11b^{lo}F4/80^{lo} (P2) cells relative to CD11b^{hi}F4/80^{hi} (P1) cells in CCR2$^{+/+}$ mice were assessed (mean ± SEM; n = 4 biological replicates). *C*: Representative images of H-E–stained CD11b^{hi}F4/80^{hi} (P1) and CD11b^{lo}F4/80^{lo} (P2) cells. *P < 0.05 compared with CD11b^{hi}F4/80^{hi}. (A high-quality color representation of this figure is available in the online issue.)

ACKNOWLEDGMENTS

This work was supported by National Institutes of Health (NIH) Grant HL-089466 and a supplement to this grant to D.A.G. D.A.G. also has received support from Molecular Endocrinology Training Grant NIH DK-07563-23. A.H.H. has received the American Diabetes Association Career Development Award 1-07-CD-10. Flow cytometry experiments were performed in the Vanderbilt Flow Cytometry Shared Resource, supported by the Vanderbilt Digestive Disease Research Center (DK-058404).

No potential conflicts of interest relevant to this article were reported.

D.A.G. collected and analyzed the data and wrote the manuscript. A.K., J.S.O., E.K.A., and C.D.W. assisted with data collection and reviewed the manuscript. W.K.G. assisted with data collection. A.H.H. assisted with data analysis, provided important intellectual contributions, and wrote and edited the manuscript.

The authors thank the Major Laboratory (Vanderbilt) for their assistance with flow cytometry and ELISA experiments, the Southard-Smith Laboratory (Vanderbilt) for their assistance with RNA isolation from sorted cells, and Laura Price from the VUMC Cytopathology Laboratory for her assistance with cytospins.

REFERENCES

1. Ouchi N, Parker JL, Lugus JJ, Walsh K. Adipokines in inflammation and metabolic disease. Nat Rev Immunol 2011;11:85–97
2. Donath MY, Shoelson SE. Type 2 diabetes as an inflammatory disease. Nat Rev Immunol 2011;11:98–107
3. Monteiro R, Azevedo I. Chronic inflammation in obesity and the metabolic syndrome. Mediators Inflamm. 14 July 2010 [Epub ahead of print]
4. Weisberg SP, McCann D, Desai M, Rosenbaum M, Leibel RL, Ferrante AW Jr. Obesity is associated with macrophage accumulation in adipose tissue. J Clin Invest 2003;112:1796–1808
5. Xu H, Barnes GT, Yang Q, et al. Chronic inflammation in fat plays a crucial role in the development of obesity-related insulin resistance. J Clin Invest 2003;112:1821–1830
6. Lumeng CN, DelProposto JB, Westcott DJ, Saltiel AR. Phenotypic switching of adipose tissue macrophages with obesity is generated by spatiotemporal differences in macrophage subtypes. Diabetes 2008;57:3239–3246
7. Charo IF, Ransohoff RM. The many roles of chemokines and chemokine receptors in inflammation. N Engl J Med 2006;354:610–621
8. Boring L, Gosling J, Chensue SW, et al. Impaired monocyte migration and reduced type 1 (Th1) cytokine responses in C-C chemokine receptor 2 knockout mice. J Clin Invest 1997;100:2552–2561
9. Tsou CL, Peters W, Si Y, et al. Critical roles for CCR2 and MCP-3 in monocyte mobilization from bone marrow and recruitment to inflammatory sites. J Clin Invest 2007;117:902–909
10. Geissmann F, Manz MG, Jung S, Sieweke MH, Merad M, Ley K. Development of monocytes, macrophages, and dendritic cells. Science 2010;327:656–661
11. Weisberg SP, Hunter D, Huber R, et al. CCR2 modulates inflammatory and metabolic effects of high-fat feeding. J Clin Invest 2006;116:115–124
12. Kanda H, Tateya S, Tamori Y, et al. MCP-1 contributes to macrophage infiltration into adipose tissue, insulin resistance, and hepatic steatosis in obesity. J Clin Invest 2006;116:1494–1505
13. Ito A, Suganami T, Yamauchi A, et al. Role of CC chemokine receptor 2 in bone marrow cells in the recruitment of macrophages into obese adipose tissue. J Biol Chem 2008;283:35715–35723

14. Tamura Y, Sugimoto M, Murayama T, et al. Inhibition of CCR2 ameliorates insulin resistance and hepatic steatosis in db/db mice. Arterioscler Thromb Vasc Biol 2008;28:2195–2201
15. Inouye KE, Shi H, Howard JK, et al. Absence of CC chemokine ligand 2 does not limit obesity-associated infiltration of macrophages into adipose tissue. Diabetes 2007;56:2242–2250
16. Yang SJ, IglayReger HB, Kadouh HC, Bodary PF. Inhibition of the chemokine (C-C motif) ligand 2/chemokine (C-C motif) receptor 2 pathway attenuates hyperglycaemia and inflammation in a mouse model of hepatic steatosis and lipoatrophy. Diabetologia 2009;52:972–981
17. Coenen KR, Gruen ML, Lee-Young RS, Puglisi MJ, Wasserman DH, Hasty AH. Impact of macrophage toll-like receptor 4 deficiency on macrophage infiltration into adipose tissue and the artery wall in mice. Diabetologia 2009;52:318–328
18. Surmi BK, Webb CD, Ristau AC, Hasty AH. Absence of macrophage inflammatory protein-1alpha does not impact macrophage accumulation in adipose tissue of diet-induced obese mice. Am J Physiol Endocrinol Metab 2010;299:E437–E445
19. Pfaffl MW. A new mathematical model for relative quantification in real-time RT-PCR. Nucleic Acids Res 2001;29:e45
20. Gower RM, Wu H, Foster GA, et al. CD11c/CD18 expression is upregulated on blood monocytes during hypertriglyceridemia and enhances adhesion to vascular cell adhesion molecule-1. Arterioscler Thromb Vasc Biol 2011;31:160–166
21. Wu H, Perrard XD, Wang Q, et al. CD11c expression in adipose tissue and blood and its role in diet-induced obesity. Arterioscler Thromb Vasc Biol 2010;30:186–192
22. Ablamunits V, Weisberg SP, Lemieux JE, Combs TP, Klebanov S. Reduced adiposity in ob/ob mice following total body irradiation and bone marrow transplantation. Obesity (Silver Spring) 2007;15:1419–1429
23. Peters W, Dupuis M, Charo IF. A mechanism for the impaired IFN-gamma production in C-C chemokine receptor 2 (CCR2) knockout mice: role of CCR2 in linking the innate and adaptive immune responses. J Immunol 2000;165:7072–7077
24. Szymczak WA, Deepe GS Jr. The CCL7-CCL2-CCR2 axis regulates IL-4 production in lungs and fungal immunity. J Immunol 2009;183:1964–1974
25. Kuziel WA, Morgan SJ, Dawson TC, et al. Severe reduction in leukocyte adhesion and monocyte extravasation in mice deficient in CC chemokine receptor 2. Proc Natl Acad Sci USA 1997;94:12053–12058
26. Sonoda KH, Yoshimura T, Egashira K, Charo IF, Ishibashi T. Neutrophil-dominant experimental autoimmune uveitis in CC-chemokine receptor 2 knockout mice. Acta Ophthalmol 2011;89:e180–e188
27. Obstfeld AE, Sugaru E, Thearle M, et al. C-C chemokine receptor 2 (CCR2) regulates the hepatic recruitment of myeloid cells that promote obesity-induced hepatic steatosis. Diabetes 2010;59:916–925
28. Chomarat P, Banchereau J, Davoust J, Palucka AK. IL-6 switches the differentiation of monocytes from dendritic cells to macrophages. Nat Immunol 2000;1:510–514
29. MacDonald KP, Palmer JS, Cronau S, et al. An antibody against the colony-stimulating factor 1 receptor depletes the resident subset of monocytes and tissue- and tumor-associated macrophages but does not inhibit inflammation. Blood 2010;116:3955–3963
30. Fantuzzi L, Borghi P, Ciolli V, Pavlakis G, Belardelli F, Gessani S. Loss of CCR2 expression and functional response to monocyte chemotactic protein (MCP-1) during the differentiation of human monocytes: role of secreted MCP-1 in the regulation of the chemotactic response. Blood 1999;94:875–883
31. Struthers M, Pasternak A. CCR2 antagonists. Curr Top Med Chem 2010;10:1278–1298
32. Kang YS, Cha JJ, Hyun YY, Cha DR. Novel C-C chemokine receptor 2 antagonists in metabolic disease: a review of recent developments. Expert Opin Investig Drugs 2011;20:745–756